Effect of pH and Copper(II) on the Conformation Transitions of Silk Fibroin Based on EPR, NMR, and Raman Spectroscopy†

Xiao-Hong Zong,‡ Ping Zhou,*,‡ Zheng-Zhong Shao,‡ Shi-Ming Chen,§ Xin Chen,‡ Bing-Wen Hu,‡ Feng Deng,|| and Wen-Hua Yao§

The Key Laboratory of Molecular Engineering of Polymers, Department of Macromolecular Science, and The Analytical Measurement Center, Fudan University, Shanghai 200433, China, and The State Key Laboratory of Magnetic Resonance and Atomic and Molecular Physics, Wuhan Institute of Physics and Mathematics, The Chinese Academy of Sciences, Wuhan 430071, China

Received March 19, 2004; Revised Manuscript Received July 4, 2004

ABSTRACT: Much attention has been paid to the natural mechanism of silkworm spinning due to the impressive mechanical properties of the natural fibers. Our results in the present work show that the fractional changes of the conformational components in regenerated silk fibroin (SF) extracted from *Bombyx mori* fibers is remarkably pH- and Cu(II)-dependent as demonstrated by Cu(II) EPR, ^{13}C NMR, and Raman spectroscopy. Cu(II) coordination atoms in SF are changed from four nitrogens to two nitrogens and two oxygens as well as to one nitrogen and three oxygens when the pH is lowered from 8.0 to 4.0. The addition of a given amount of Cu(II) into a SF solution could induce efficiently the SF conformational fractional change from silk I, a soluble helical conformation, to silk II, an insoluble β-sheet conformation. This behavior is strikingly similar to that seen in prion protein and amyloid β-peptide. On the basis of the similarity in the relevant sequence in SF to the octapeptide PHGGGWGQ in PrP, we suggest that at basic and neutral pH polypeptide AHGGYSGY in SF may form a 1:1 complex with Cu(II) by coordination of imidazole N_π of His together with two deprotonated main-chain nitrogens from two glycine residues and one nitrogen or oxygen from serine. Such a type of coordination may make the interaction between two adjacent β-form polypeptide chains more difficult, thereby leading to an amorphous structure. Under weakly acidic conditions, however, Cu(II)−amide linkages may be broken and Cu(II) may switch to bind two N_τ from two histidines in adjacent peptide chains, forming an intermolecular His(N_τ)−Cu(II)−His(N_τ) bridge. This type of coordination may induce β-sheet formation and aggregation, leading to a crystalline structure.

Recently, more and more attention has been paid to natural silk, which is produced by a wide variety of insects, such as silkworms and spiders (*1*−*6*). Although silk's impressive mechanical properties are closely related to the primary amino acid sequence, the silk spinning conditions, such as temperature, pH, ionic strength, solvent composition, and mechanical stress, are possibly more important (*7*−*10*). Indeed, it is interesting to note that a spider or silkworm produces such strong fibers merely at ambient temperature and pressure from weakly acidic aqueous solution and in the presence of a small amount of metal ions (*9*−*18*). Among the numerous silks, *Bombyx mori* silkworm silk has been extensively studied. The primary amino acid sequence of its heavy chain, a predominating polypeptide in silk fibroin (SF),[1] consists of two amino acid motifs. One is composed of the repeated -(Gly-Ala-Gly-Ala-Gly-Ser)$_8$- amino acid sequences, and the other is composed of the unrepeated amino acid sequences (*19*). It has been accepted that there are two types of crystalline states in the former motif, namely, silk I, a helical conformation, and silk II, an antiparallel β-sheet conformation (*11*, *20*, *21*). During the natural silk spinning from the spinneret of a silkworm, the conformation of SF converts from helical to β-sheet (*8*).

Magoshi et al. (*8*, *10*) found that the pH changed gradually in the lumen of the *B. mori* silkworm from neutral (pH 6.9) in the posterior division to weakly acidic (pH 4.8) in the anterior division adjacent to the spinneret. At the same time, the concentration of inorganic ions such as Ca(II), K(I), and Mg(II) varied within each division of the silk gland (*8*, *22*), which promotes the transition from gel to solution state and the silk fiber formation (*10*). Moreover, our previous work (*23*) demonstrated that the copper content in the *B. mori* silk gland increased from the posterior part [$(0.31 \pm 0.24) \times 10^{-3}$ mg of Cu/g of SF] to the anterior part [$(1.3 \pm 0.24) \times 10^{-3}$ mg of Cu/g of SF], and it was much higher in native

† Supported by grants from the NSFC (20274009 and 29974004) and from the State Key Laboratory of Magnetic Resonance and Atomic and Molecular Physics, China.

* To whom correspondence should be addressed. Phone: +86-21-55664038. Fax: +86-21-65640293. E-mail: pingzhou@fudan.edu.cn.

‡ The Key Laboratory of Molecular Engineering of Polymers, Department of Macromolecular Science, Fudan University.

§ The Analytical Measurement Center, Fudan University.

|| Wuhan Institute of Physics and Mathematics, The Chinese Academy of Sciences.

[1] Abbreviations: SF, silk fibroin; NMR, nuclear magnetic resonance; EPR, electronic paramagnetic resonance; CD, circular dichroism; PrP, prion protein; Aβ, amyloid β-peptide; PIXE, proton-induced X-ray emission; His, histidine.

10.1021/bi049455h CCC: $27.50
Published on Web 08/28/2004

silk fiber [$(4.99 \pm 0.73) \times 10^{-3}$ mg of Cu/g of SF] than in the silk gland. We also found that a given amount of Cu(II) could induce the fractional change of conformation from silk I to silk II in regenerated SF membrane (*14*). Meanwhile, we had also observed that the conformation transition of SF in solution followed a nucleation-dependent aggregation mechanism (*24*). How the metallic ions, especially Cu(II) ions, and pH impact on the SF conformation transition, that is, what mechanism is involved in the conformation conversion, still remains unclear up to now. Cu(II) is known to play a vital role in the folding and refolding processes in many proteins and polypeptides. For example, the cellular isoform of prion protein (PrP) undergoes a conformational transition from α-helix-rich to β-sheet-rich structure induced by the presence of Cu(II) in weakly acidic solutions. Abnormal aggregation of the β-sheet-rich isoform, PrP^{sc}, causes the fatal neurodegenerative diseases including Creutzfeldt−Jakob disease in humans and spongiform encephalopathy in animals (*25*−*29*). Also, amyloid β-peptide (Aβ), a major constituent of senile plaques in the brains of patients with Alzheimer's disease, aggregates and accumulates to form amyloid fibrils possibly induced by Cu(II) at mildly acidic pH (*30*, *31*).

These strikingly similarities in pH- and Cu(II)-dependent protein refolding between SF and PrP or Aβ-peptide lead us to attempt to reveal the refolding mechanism of SF induced by pH and Cu(II) ions in present work. Cu(II) EPR spectroscopy was used to determine the coordination modes of Cu(II)−SF complexes, and Raman and ^{13}C solid-state NMR spectroscopies were used to determine qualitatively and quantitatively the SF conformations. The relationship between pH, coordination modes of Cu(II)−SF complexes, and SF conformations is assessed here. These findings will be significant to medical research, on one hand, as SF, extracted in large amounts from *B. mori* silkworm gland, could be a proper model to study the mechanisms and medicaments for the nervous system disease. On the other hand, these results will serve as guidance for the controllable design of high-performance materials as silk fibers.

MATERIALS AND METHODS

Sample Preparation. Raw *B. mori* silk fiber of the cocoon was treated with boiling aqueous Na_2CO_3 (0.5 wt %) solution for half an hour to remove the sericin coating on the raw silk fiber. The degummed silk fibers were washed with copious amounts of water and allowed to air-dry at room temperature. The regenerated SF solution was prepared by dissolving 8 g of degummed silk into a 100 mL 9.3 M LiBr solution for 1 h at room temperature. This resulting solution was dialyzed against deionized water at ambient temperature for 3 days to remove LiBr. The deionized water was changed every 3 h during dialysis, and an ∼3% (w/v) regenerated silk fibroin bulk solution was obtained.

A series of Cu(II)−SF solutions were prepared by mixing of the 3% (w/v) regenerated SF solution and a certain amount of aqueous $CuCl_2$ solution. The pH of the solutions was adjusted to the desired value by 0.01 M aqueous hydrochloric acid (HCl) and sodium hydroxide (NaOH). The solution was cast on a polystyrene surface and dried at room temperature for 3 days.

The original content of Cu(II) ions in the regenerated SF is 0.018 ± 0.002 mg of Cu/g of SF as detected by PIXE (*14*). This value is higher than that in silk gland and silk fiber determined previously (*23*) possibly because all of the sericin has been removed in the regenerated SF. The added Cu(II) content in the series of prepared Cu(II)−SF complex membranes is 0, 5, 10, 20, 35, 50, and 100 times the original Cu(II) content in the regenerated SF; that is, the added Cu(II) content in the prepared Cu(II)−SF complex membranes is 0, 0.09, 0.18, 0.36, 0.63, 0.9, and 1.8 mg of Cu/g of SF, respectively.

EPR Experiments. EPR spectra of Cu(II)−SF complex membranes were recorded on a Bruker ER 200D-SRC spectrometer equipped with an Aspect 3000 data system. The experimental temperature was 100 K as controlled by a Bruker ER 4111VT temperature control system. All of the samples were allowed to equilibrate after cooling to the required temperature. A 20 mW microwave power at a frequency of 9.67 GHz was used with a modulation amplitude of 1 G and frequency of 100 kHz. All EPR spectra were recorded at a sweep width of 1200 G (Figure 1). The measured *g*-values were corrected against a known *g*-standard sample, DPPH (diphenylpicrylhydrazyl, $g = 2.0036$). The EPR spectra were simulated (Figure 2) with the EprSimu program developed in our group based on the second-order perturbation theory (*32*).

Raman Spectroscopy. Raman spectra were recorded using a Dilor LabRam-1B spectrometer, operating at a resolution of 1 cm^{-1}. The Spectra Physics Model 164 argon ion laser was operated at 632.8 nm with about 6 mW of power.

^{13}C CP-MAS NMR and Spectral Simulation. ^{13}C CP-MAS NMR measurements were performed on the prepared membranes using a Varian InfinityPlus-400 NMR spectrometer, operating at 100 MHz with a CP contact time of 1 ms and pulse repeat time of 2 s, which is long enough for sufficient relaxation of the interested nucleus. Over 1000 scans were accumulated with a 7.5 mm rotor at a magic angle spinning rate of 5 kHz and high-power ^1H decoupling during signal acquisition with a ^1H 90° pulse width of 4.0 μs. Chemical shifts were reported as referred to the methyl carbon (17.4 ppm) in hexamethylbenzene as an external reference. The NMR peak of C_β (chemical shifts between 10 and 30 ppm) for alanine residues was simulated using Gaussian functions to quantitatively analyze the relevant contents of the conformation components (Figure 5) as this peak provides a sensitive discrimination between silk I and silk II as well as other secondary structures in fibroin (*20*, *33*, *34*).

RESULTS

pH-Dependent Cu(II) Coordination Mode with Regenerated SF. Figure 1 shows the EPR spectra of the Cu(II)−SF complex membranes prepared with an added Cu(II) concentration of 1.8 mg of Cu/g of SF at pH 4.0, 5.2, 6.9, and 8.0, respectively. It is evident that the spectra are remarkably sensitive to pH variation. The quadruplex hyperfine splittings are shifted to upfield in the low-field region, a parallel region in the spectrum, as the pH is increased from 4.0 to 8.0. The EPR spectra show characteristic type II Cu(II)−protein complexes with tetragonal coordination geometry, either as square planar or as square planar with a weak longitudinal axial ligand (*35*). Theoretically, the *g*-factor of EPR characterizes the detailed information on the intramolecular interactions. The EPR spectrum for an axial symmetric Cu(II)

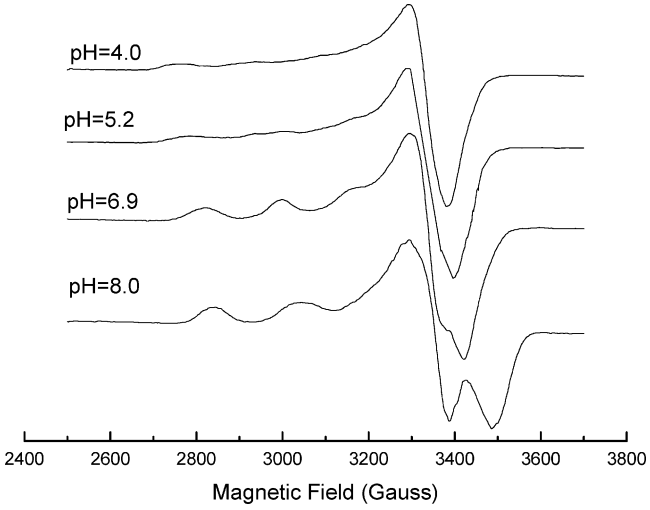

FIGURE 1: EPR spectra of the Cu(II)−SF complexes (membranes) prepared at different pH values with an added Cu(II) concentration of 1.8 mg of Cu/g of SF. All spectra were collected at 100 K, $\nu_0 = 9.67$ GHz, and a sweep width of 1200 G.

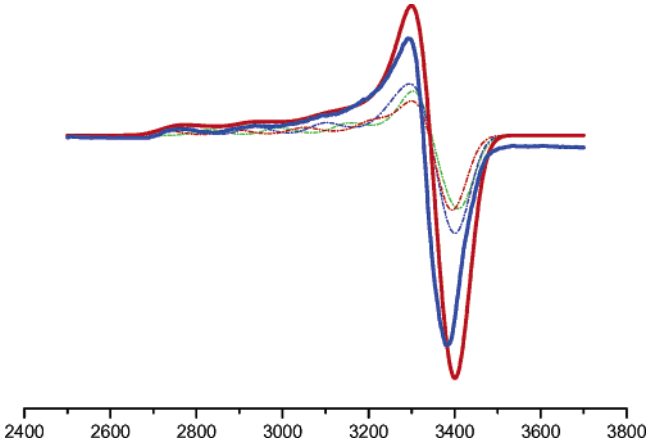

FIGURE 2: Experimental and simulated EPR spectra of the Cu(II)−SF complex membranes prepared in a pH 5.2 SF solution with an added Cu(II) concentration of 1.8 mg of Cu/g of SF: experimental spectrum (bold solid red line), simulated spectrum (bold solid blue line), and deconvoluted component traces (component 1, blue dashed line; component 2, red dashed line; component 3, green dashed line). The relevant error in all reported coordination contents is less than 2%.

complex shows a strong resonance at the higher field region with $g_\perp$ and a weak resonance at the lower field region with $g_{||}$. The hyperfine coupling constants, $A_\perp$ and $A_{||}$, arise from the perpendicular and parallel interactions, respectively, between the nuclear magnetic moment of Cu(II) and that of the electronic spin. The $g_{||}$ and $A_{||}$ extracted from the parallel region in the spectrum are sensitive to the changes in the ligands around the environment of Cu(II) and can give insight into the type of coordination involved (*35*).

The EPR spectra of Cu(II)−SF complexes were simulated using the EprSimu program. Figure 2 shows an example of the experimental and simulated spectra and deconvoluted traces for a membrane prepared in a solution with a pH of 5.2 and an added Cu(II) concentration of 1.8 mg of Cu/g of SF. The peak resonance positions and intensities in the simulated spectrum (bold solid blue line in Figure 2) in the parallel region are in good agreement with those in the experimental spectrum (bold solid red line). Table 1 summarizes the extracted parameters from the deconvoluted EPR traces, such as $A_{||}$, $A_\perp$, $g_{||}$, and $g_\perp$, and the deconvoluted components for the Cu(II)−SF complexes prepared with an added 1.8 mg of Cu/g of SF at different pH values.

The most likely ligands coordinating to Cu(II) in our studied samples are oxygen and nitrogen atoms, based on the obtained $A_{||}$ and $g_{||}$ values (*36*, *37*). In general, when $A_{||} > 160 \times 10^{-4}$ cm^{-1} and $g_{||} < 2.30$, the ligand is supposed to be nitrogen coordinated, while when $A_{||} < 180 \times 10^{-4}$ cm^{-1} and $g_{||} > 2.30$, it is supposed to be the oxygen atom coordinating to Cu(II). In addition, the value of $A_{||}$ would be extremely small if sulfur were the coordination atom with Cu(II) (*36*, *37*). It has been suggested that the ratio $g_{||}/A_{||}$ can be viewed as an empirical measure of the amount of the tetrahedral distortion in Cu(II) complexes (*38*). If this ratio is in the range of 105−135 cm, a square-planar geometry is suggested (*39*, *40*). The ratios of $g_{||}/A_{||}$ shown in Table 1 therefore confirm the Cu(II) bonding with four ligands in an approximately square-planar configuration here (*39*, *40*). At a pH of 8.0 (Figure 1 and Table 1), the spectrum shows quadruplex hyperfine splitting with $g_{||} = 2.200$ and $A_{||} = 202 \times 10^{-4}$ cm^{-1} (197 G). According to the Peisach−Blumberg (PB) plot (*35*), these values fall in the range expected for a four-nitrogen coordination mode (Cu−4N). At a pH of 6.9, the quadruplex hyperfine splitting shifts to a higher field with $g_{||} = 2.235$ and $A_{||} = 190 \times 10^{-4}$ cm^{-1} (182 G), for which we propose a three-nitrogen and one-oxygen coordination mode (Cu−3N1O), but Cu−4N or Cu−2N2O coordination could not be ruled out (*35*). At a pH of 5.2, three sets of hyperfine splittings are superposed in the spectra, namely, at $g_{||} = 2.250$ and $A_{||} = 168 \times 10^{-4}$ cm^{-1} (160 G), which we refer to as the two-nitrogen and two-oxygen coordination mode (Cu−2N2O, component 1, 40%), at $g_{||} = 2.327$ and $A_{||} = 172 \times 10^{-4}$ cm^{-1} (158 G) to a one-nitrogen and three-oxygen coordination mode (Cu−1N3O, component 2, 30%), and at $g_{||} = 2.290$ and $A_{||} = 173 \times 10^{-4}$ cm^{-1} (162 G) to a second (different) one-nitrogen and three-oxygen coordination (Cu−1N3O, component 3, 30%), respectively. Finally, at a pH of 4.0, two sets of hyperfine splittings are observed superposed in the spectra with values of $g_{||} = 2.256$ and $A_{||} = 168 \times 10^{-4}$ cm^{-1} (160 G) (Cu−2N2O, component 1′) and $g_{||} = 2.317$ and $A_{||} = 177 \times 10^{-4}$ cm^{-1} (164 G) (Cu−1N3O, component 2′), respectively.

Concentration-Dependent Cu(II) Coordination with Regenerated SF. We also recorded the EPR spectra of a series of samples with different contents of Cu(II) prepared at various pH values as above. Because it is difficult to observe the EPR signal when the Cu(II) concentration is too low, the spectra were only recorded when added Cu(II) concentrations varied from 0.18 to 1.8 mg of Cu/g of SF. Compared with the spectra of Cu(II)−SF complexes with added Cu(II) of 1.8 mg of Cu/g of SF (Table 1), the resulting EPR spectra and extracted EPR-related parameters, $A_{||}$, $A_\perp$, $g_{||}$, and $g_\perp$, exhibit no obvious changes as the Cu(II) contents are varied (figures and simulated parameters not shown here). However, at a pH of 5.2 and 4.0, the contents of the different coordination modes are changed as Cu(II) concentration is increased. For example, at a pH of 5.2, when the added Cu(II) concentration is lower than 0.36 mg of Cu/g of SF, the amount of the coordination mode Cu−2N2O is 50%, while when the added Cu(II) content is increased further from 0.63 mg of Cu/g of SF, the content of this coordination mode

Table 1: Summary of EPR Parameters and Coordination Modes for Cu(II)−SF Complexes Prepared at Different pH Values with an Added Cu(II) Concentration of 1.8 mg of Cu/g of SF

pH	component	$A_{\|\|}$[a] G	$A_{\|\|}$[a] 10^{-4} cm^{-1}	$A_{\perp}$[a] G	$A_{\perp}$[a] 10^{-4} cm^{-1}	$g_{\|\|}$[b]	$g_{\perp}$[b]	$g_{\|\|}/A_{\|\|}$	relevant contents (%)[c]	coordination modes
8.0		197	202	18	17	2.200	2.063	109	100	Cu−4N
6.9		182	190	16	15	2.235	2.068	117	100	Cu−3N1O
5.2	1	160	168	10	10	2.250	2.063	134	40	Cu−2N2O
	2	158	172	10	10	2.327	2.063	135	30	Cu−1N3O
	3	162	173	10	10	2.290	2.063	132	30	Cu−1N3O
4.0	1′	160	168	20	20	2.256	2.094	134	50	Cu−2N2O
	2′	164	177	20	20	2.317	2.094	131	50	Cu−1N3O

[a] A (cm^{-1}) = (0.46686 × 10^{-4})gA (gauss), and the absolute error in all reported A values is less than ±2G. [b] Absolute error in g-values is ±0.002. [c] Relevant error in all reported contents is less than 2%.

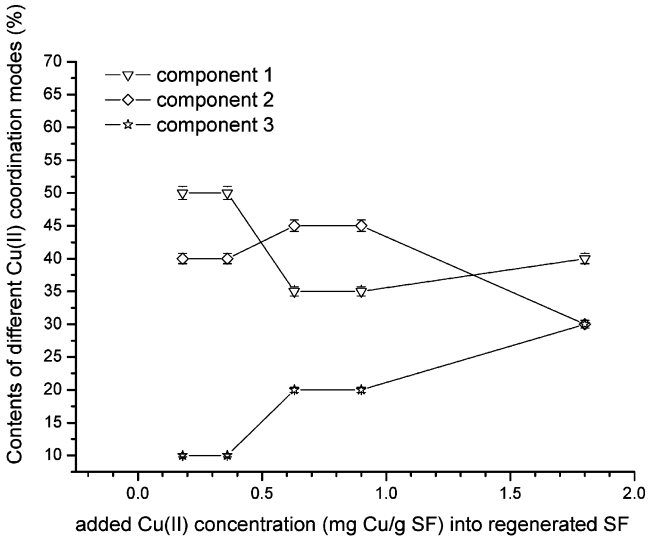

FIGURE 3: Dependence of Cu(II) coordination modes determined by EPR on the added Cu(II) concentrations in the Cu(II)−SF complex membranes prepared at pH 5.2. The relevant error in all reported coordination contents is less than 2%.

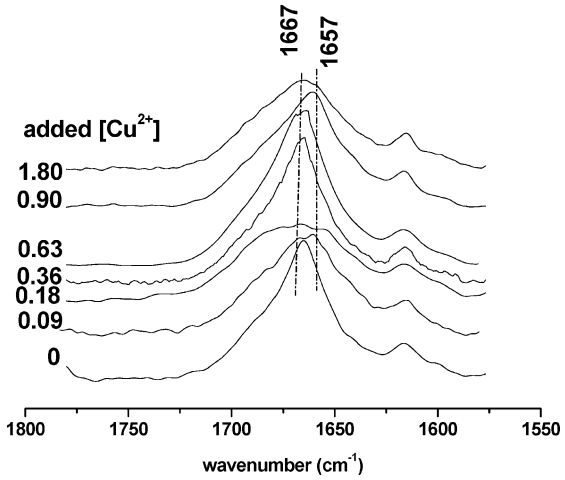

FIGURE 4: Raman spectra of a series of SF membranes prepared at a pH of 5.2 with added Cu(II) concentrations of 0, 0.09, 0.18, 0.36, 0.63, 0.90, and 1.80 mg of Cu/g of SF.

decreases, and the other two coordination modes increase (Figure 3).

Conformation Studied by Raman Spectroscopy. The Raman spectrum of protein in the amide I region (1600−1700 cm^{-1}) shows high intensity and little interference from other group vibrations and is susceptive to the protein conformation changes (*41*, *42*). Although there are other Raman bands, for example, the amide II region (1400−1500 cm^{-1}) and amide III region (1200−1300 cm^{-1}), often used as marker bands for identifying the protein structure, these bands suffer interference from bands from the side groups of amino acids in silk fibroin and make it difficult to analyze the conformation transition of the protein (*43*). Thus the amide I region has been used widely to estimate the secondary structure elements of proteins (*44*) as well as silk fibroin (*45*, *46*). In general, a peak at 1670 ± 5 cm^{-1} is ascribed to β-sheet, at 1660 ± 5 cm^{-1} to silk I and/or random coil and at 1654 ± 5 cm^{-1} to α-helix (*43*).

Raman spectra of regenerated SF membranes prepared at a pH of 5.2 in the presence of Cu(II) are shown in Figure 4. They demonstrate that the addition of Cu(II) obviously influences the SF conformation transition in Cu(II)−SF complex membranes. Upon addition of Cu(II) from 0.09 to 0.18 mg of Cu/g of SF, the amide I band of SF becomes broader, suggesting that the conformation of SF dramatically changes. However, when the concentration of Cu(II) is increased to 0.36 mg of Cu/g of SF, the amide I band of the SF shift from 1657 to 1667 cm^{-1} means that the β-sheet conformation is getting an increase in SF. With further addition of Cu(II), i.e., 0.63 and 1.80 mg of Cu/g of SF, the strongest peak moves to 1657 cm^{-1} or even broadens again.

Contents of Conformations Analyzed by the Simulation of the ^{13}C NMR Spectrum. To quantitatively analyze the components of the conformations formed upon changing the Cu(II) concentration, we simulated the ^{13}C CP-MAS solid-state NMR spectra. The experimental and simulated NMR spectra and deconvoluted traces for the alanine C_β nucleus at a chemical shift between 5 and 30 ppm are shown in Figure 5, and the extracted chemical shifts and contents of the corresponding conformation are summarized in Table 2. Originally we simulated the NMR spectrum with two components at chemical shifts of 17.0 ± 0.5 and 20.0 ± 0.5 ppm (not shown here), but it did not fit well with the experimental spectrum. However, we found that there were more than two different conformations in our studied samples based on the Raman spectra (Figure 4). Thus, we deconvoluted the NMR line shape with four components at chemical shifts of 15.0 ± 0.5, 17.0 ± 0.5, 20.0 ± 0.5, and 21.5 ± 0.5 ppm. The analysis of the conformation contents shows that when Cu(II) content is changed from 0.09 to 0.36 mg of Cu/g of SF at a pH of 5.2, the silk fibroin conformation undergoes fractionally a transition from typical silk I structure (17.0 ± 0.5 ppm) to typical silk II structure (20.0 ± 0.5 ppm); that is, the typical silk II content increases from 26%

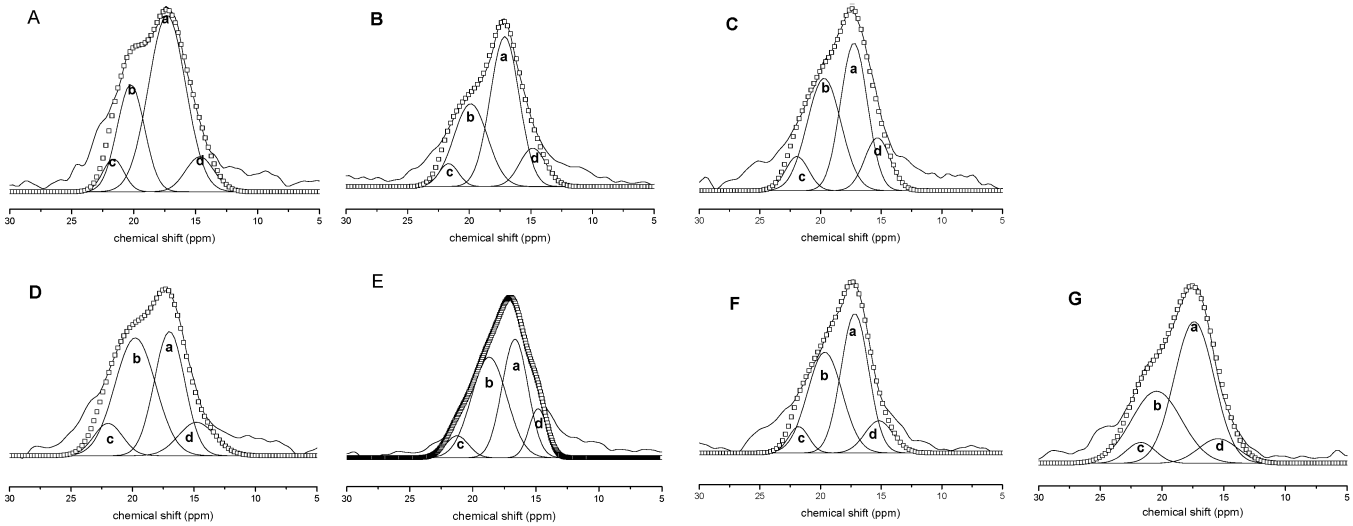

FIGURE 5: ^{13}C CP-MAS NMR spectra (solid line), simulated spectra (hollow squares), and their deconvoluted traces for alanine C_β. A, B, C, D, E, F, and G are the membranes prepared from regenerated fibroin in a pH 5.2 fibroin solution with added Cu(II) concentrations of 0, 0.09, 0.18, 0.36, 0.63, 0.90, and 1.80 mg of Cu/g of SF, respectively. The deconvoluted traces give (a) typical silk I (17.0 ± 0.5 ppm), (b) typical silk II (20.0 ± 0.5 ppm), (c) silk II related intermediate (21.5 ± 0.5 ppm), and (d) silk I related intermediate (15.0 ± 0.5 ppm).

Table 2: Summary of Simulated Results of ^{13}C NMR Spectra for Membranes Prepared at pH 5.2 in Regenerated Silk Fibroin Solutions with Different Added Cu(II) Concentrations

added Cu(II) (mg of Cu/ g of SF) into regenerated silk fibrion	relevant conformation contents (%)[a]					
	(a) typical silk I	(b) typical silk II	(c) silk II related inter-mediate	(d) silk I related inter-mediate	(a + d) total silk I	(b + c) total silk II
0	59	26	6	9	65	35
0.09	49	32	7	12	61	39
0.18	40	39	8	13	53	47
0.36	35	45	9	11	46	54
0.63	38	44	7	11	49	51
0.90	44	40	6	10	54	46
1.80	52	33	9	6	58	42

[a] The relevant error in all reported conformation contents is less than 2%.

Table 3: Summary of Simulated Results of ^{13}C NMR Spectra for Membranes Prepared at pH 6.9 in Regenerated Silk Fibroin Solutions with Different Added Cu(II) Concentrations

added Cu(II) (mg of Cu/ g of SF) into regenerated silk fibrion	relevant conformation contents (%)[a]					
	(a) typical silk I	(b) typical silk II	(c) silk II related inter-mediate	(d) silk I related inter-mediate	(a + d) total silk I	(b + c) total silk II
0	61	20	9	10	71	29
0.09	52	25	10	13	65	35
0.18	50	30	11	9	59	41
0.36	40	32	11	17	57	43
0.63	51	37	8	4	55	45
0.90	53	22	7	18	71	29
1.80	66	20	8	6	72	28

[a] The relevant error in all reported contents is less than 2%.

Table 4: Summary of Simulated Results of ^{13}C NMR Spectra for Membranes Prepared at pH 8.0 in Regenerated Silk Fibroin Solutions with Different Added Cu(II) Concentrations

added Cu(II) (mg of Cu/ g of SF) into regenerated silk fibrion	relevant conformation contents (%)[a]					
	(a) typical silk I	(b) typical silk II	(c) silk II related inter-mediate	(d) silk I related inter-mediate	(a + d) total silk I	(b + c) total silk II
0	71	17	5	7	78	22
0.09	61	19	9	11	72	28
0.18	52	24	14	10	62	38
0.36	47	29	11	13	60	40
0.63	45	34	9	12	57	43
0.90	65	18	10	7	72	28
1.80	67	12	13	8	75	25

[a] The relevant error in all reported contents is less than 2%.

to 45% whereas that of typical silk I decreases from 59% to 35% (Table 2). At the same time, there are another two components present at chemical shifts of 15.0 ± 0.5 and 21.5 ± 0.5 ppm, respectively. On the basis of previous reports (*33*, *47*−*50*), the chemical shift at 15.0 ± 0.5 ppm is attributed to a silk I related intermediate (perhaps a distorted β-turn conformation), and the chemical shift at 21.5 ± 0.5 ppm is assigned to a silk II related intermediate, possibly a distorted β-sheet conformation. Table 2 shows that the total content of silk II (typical silk II and silk II related intermediate) increases from 35% to 54% as the concentration of Cu(II) is increased from 0.09 to 0.36 mg of Cu/g of SF. On the other hand, further addition of Cu(II) up to 1.8 mg of Cu/g of SF leads to a decrease in the total content of silk II down to 42%.

Moreover, we performed Raman and ^{13}C CP-MAS NMR experiments for the samples prepared at two more pH values of 6.9 and 8.0. Tables 3 and 4 summarize the simulated results of ^{13}C CP-MAS solid-state NMR spectra at a pH of 6.9 and 8.0, respectively (Raman spectra not shown here). The results indicate that there are also four conformations present and the trends of the fractional changes of the conformational components are similar to those at a pH of 5.2. However, the maximum silk II content is achieved at a Cu(II) content of 0.63 mg of Cu/g of SF for pH 6.9 or 8.0 as compared to a Cu(II) concentration of 0.36 mg of Cu/g of SF at a pH of 5.2.

DISCUSSION

pH-Dependent Cu(II) Coordination Modes and Sites in Cu(II)−SF Complexes. Cu(II) has been shown to have a strong affinity and can form stable complexes with biological molecules, such as copper proteins (*51*), prion proteins (*25*−*29*), amyloid β-peptides (*30*, *31*), sericin (*52*), and silk fibroin (*53*−*55*). In general, the most likely ligands coordinating with Cu(II) are histidine, tyrosine, serine, tryptophan residues, etc. (*56*).

The simulated results for the EPR spectra of Cu(II)−SF complexes at pH 8.0 and 6.9 (Table 1) indicate that the Cu(II) coordination with SF forms predominantly a square-planar complex with coordination modes of Cu−4N at a pH of 8.0 and Cu−3N1O at a pH of 6.9. As we know, the number of deprotonated nitrogens will increase at higher pH, resulting in more possibilities for Cu(II) coordination to nitrogen atoms. Evidence has indicated that an increase in $g_{||}$ would be accompanied by a decrease in $A_{||}$ if an oxygen ligand were replaced by a nitrogen (*57*). Therefore, compared with the results at pH 8.0 and 6.9, the assignments of a coordination mode of Cu−2N2O (component 1), a coordination mode of Cu−1N3O (component 2), and a coordination mode of Cu−1N3O (component 3) at a weakly acidic pH of 5.2 are reasonable. Furthermore, at a more acidic pH of 4.0 there are two coordination modes in the Cu(II)−SF complex, namely, a coordination mode of Cu−2N2O (component 1′) and a coordination mode of Cu−1N3O (component 2′). On the basis of the comparison of EPR parameters ($A_{||}$ and $g_{||}$) at pH 5.2 and 4.0 and the trend of the component change, we could suppose that coordination mode 1 at a pH of 5.2 is the same as coordination mode 1′ at a pH of 4.0 and equally coordination mode 2 at a pH of 5.2 is the same as coordination mode 2′ at a pH of 4.0. Because there is no component 3 present at a pH of 4.0, we suggest that component 3 might be an intermediate structure during the transition between component 1 and 2.

Interestingly, Cu(II) also forms similar coordination with amino acid residues in prion proteins (PrP) (*26*, *28*) and amyloid β-peptides (*30*) at different pH. It is evident that the His residues in the hydrophilic region of the peptides play an important role in the coordination of metallic ions, such as Zn(II) (*31*) and Cu(II) (*31*, *58*), thereby leading to the conformation conversion from a soluble α-helix-rich isoform to an insoluble β-sheet-rich structure. Cu(II) forms a square-planar geometry with PrP at neutral and basic pH (*25*). Miura (*28*) and Aronoff−Spencer (*26*) have proposed that, at these pH values, Cu(II) ion binds with the highly conserved octapeptide PHGGGWGQ motif in PrP (*59*−*61*) via the N_π atom of a His imidazole side chain, two deprotonated amide nitrogens from two sequential glycine (G) backbone amides, and one oxygen from the tryptophan (W) carbonyl side chain or from a water molecule (*26*), where the molar ratio of Cu(II) to His is 1:1 (*28*). Under mildly acidic condition (pH ∼6), however, the Cu(II)−amide linkage is broken, and the Cu(II) binding site of His switches from N_π to N_τ, the other nitrogen of the His, as a His(N_τ)−Cu−His(N_τ) bridge, where the molar ratio of Cu(II) to His is 0.5:1, to link two His residues in different peptide chains (*28*). Also, in amyloid β-peptide, Cu(II) induces Aβ aggregation via N_τ−metal ligation as above at mildly acidic pH (*30*). At neutral pH, Cu(II) binds to N_τ and to deprotonated amide nitrogens of the peptide main chain. The chelating of Cu(II) by His and main-chain amide groups results in a soluble Cu(II)−Aβ complex (*30*). Doorsaer et al. (*62*) did the pulse EPR and ENDOR studies for the Cu(II)-bound mPrP(23−231) complex at a pH range from 3 to 8. They demonstrate that there is no interaction between Cu(II) and nitrogen atom in the mPrP(23−231) peptide at lower pH. However, at pH 5.6 and 7.4, the interaction between Cu(II) and one or more nitrogen atoms happens.

In the amorphous region of *B. mori* silk fibroin, which links two crystalline regions, there exist three AHGGYSGY peptides in a silk fibroin heavy chain (*19*), which are similar to the peptide sequence of PHGGGWGY in PrP (*59*−*60*). The pH-dependent Cu(II) EPR and coordination modes in the Cu(II)−PrP (*26*, *28*) and Cu(II)−Aβ (*30*) complexes are strikingly similar to that of the Cu(II)−SF complexes observed here. Therefore, we suggest that there may be coordination modes and sites of Cu(II) with the amino acid residues in regenerated SF similar to those in PrP protein. At neutral pH, Cu(II) coordinates with SF as a mode of Cu−3N1O. The peptides AHGGYSGY in SF may form a complex with Cu(II) by coordination via the imidazole N_π atom of the His side chain together with two deprotonated main-chain amide nitrogens in the two glycine residues and one hydroxyl in the serine residue (see Chart 1). Under weakly acidic conditions (pH 5.2−4.0), the Cu(II) coordination mode may change to Cu−2N2O (component 1), and so the Cu(II)-binding site with His changes from N_π to N_τ to share a Cu(II) ion between two His residues of different peptide chains (see Chart 2). The coordination mode of Cu−1N3O may stem from Cu(II) binding one N_τ of the His residue and three oxygens from the carbonyl of glycine and serine residues or from water (*26*). Unfortunately, because of such a diluted Cu(II) element and low selected nitrogen atom numbers in the peptides AHGGYSGY of *B. mori* silk fibroin (molecular mass ∼390 kDa), further experimental evidence for the binding modes of Cu(II) with nitrogen atoms in SF is difficult to find.

In addition, we measured the fluorescence spectra for these complexes. The fibroin samples were excited at 274 nm and fluorescence was recorded between 290 and 400 nm for tyrosine residues, while the fibroin samples were excited at 295 nm and recorded between 300 and 450 nm for tryptophan residues. We did not observe any significant changes occurring as pH and Cu(II) concentrations changed within the given ranges. This indicates that most of the tyrosine and tryptophan residues do not coordinate with Cu(II), except for those tyrosine residues existing in peptides AHGGYSGY which were possibly involved in the binding with Cu(II). However, the amount of these peptides is very low in silk fibroin (*19*), therefore resulting in little change in fluorescence spectroscopy.

Relationship between Cu(II) Coordination Mode and SF Conformation. Both NMR and Raman spectra reported here indicate that the introduction of a given amount of Cu(II) into the silk fibroin could induce fractional changes of the conformational components from silk I to silk II, and the transition is pH-sensitive. Table 5 summarizes the relationship between the different conformation contents and coordination modes in Cu(II)−SF complexes prepared at various pH values with added Cu(II) concentration of 1.8 mg of Cu/g of SF. Our results indicate that the total silk II content

Chart 1: A Model for the Cu(II)−SF Complex at Neutral pH[a]

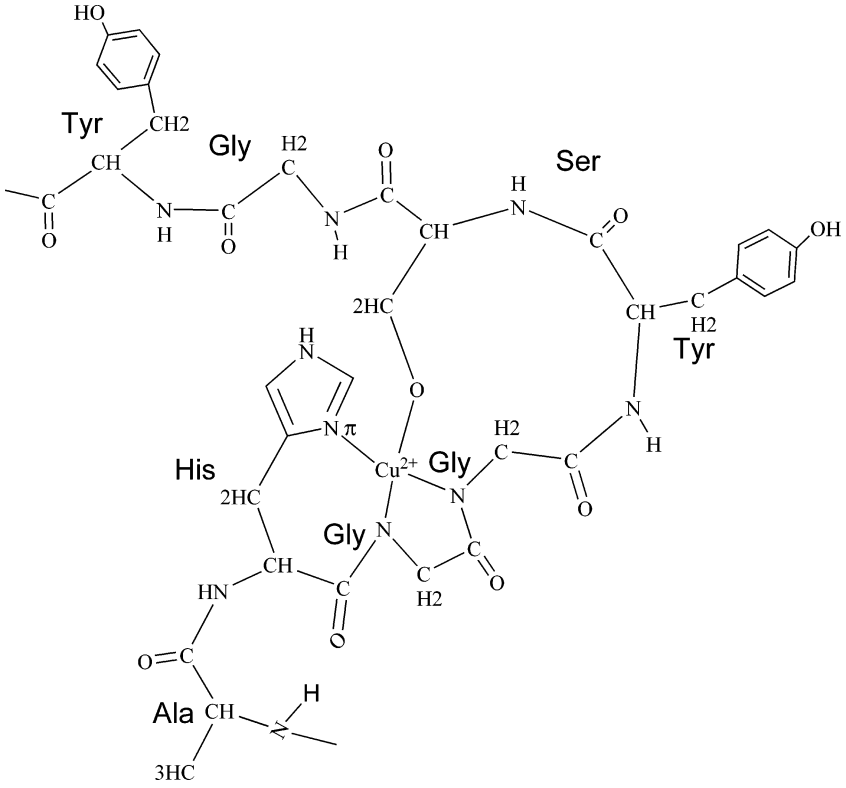

[a] Cu(II) ion is coordinated with AHGGYSGY by the N_{π} atom of a histidine residue and two depronated amide nitrogens in the two glycine residues and one oxygen atom of a serine residue.

Chart 2: A Model for the Cu(II)−SF Complex at Weakly Acidic pH[a]

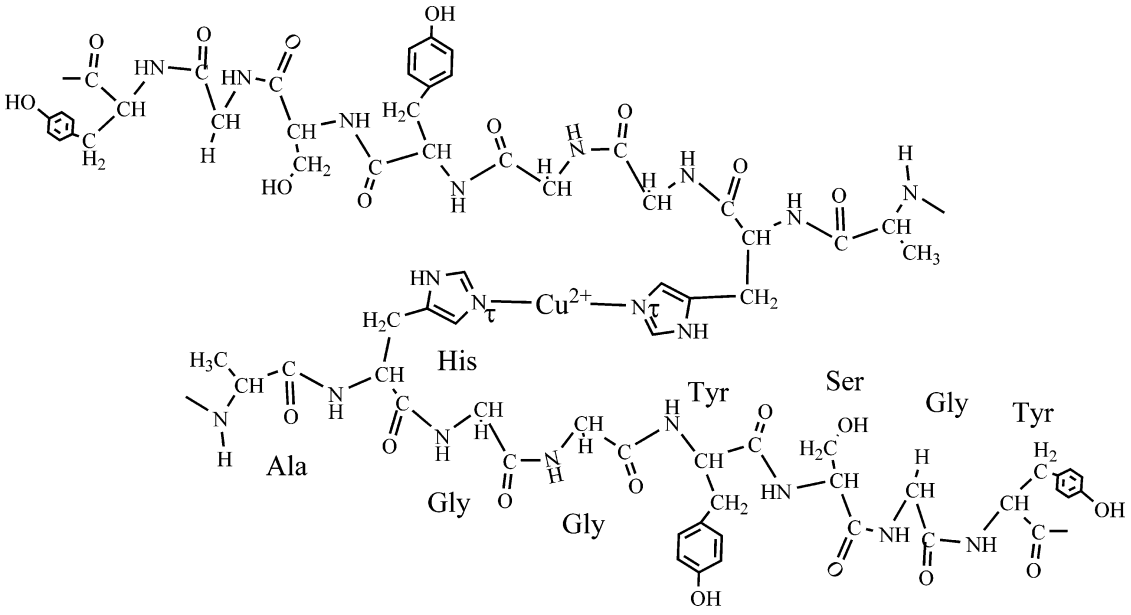

[a] Cu(II) ion is coordinated with AHGGYSGY by the His(N_{τ})−Cu(II)−His(N_{τ}) bridges.

(including typical silk II and silk II related intermediate) increases from 25% to 42% with the decrease in pH from 8.0 to 5.2, which means that the weakly acidic regenerated SF sample is more favorable for the silk II conformation. Also, interestingly, the variation in pHs within the range from 6.9 to 5.2 results in the changes of the coordination mode of the Cu(II)−SF complex from Cu−3N1O to Cu−2N2O and Cu−1N3O. Such a pH range is just in that of the silkworm gland from its posterior division to anterior division in physiologic condition (*8*). Therefore, we believe that the fractional variation of different conformational components of regenerated SF is possibly induced by the different modes of Cu(II) binding with SF at different pH values.

Notably, the silk I and silk II related conformational components are not influenced regularly by Cu(II) and pH. Unfortunately, we are not quite clear about the reasons yet. Maybe the responded conformations, distorted β-turn or distorted β-sheet, are too flexible and easily changed. The conformation change of PrP in the presence of Cu(II) as revealed by CD spectra was not consistent with α-helix or

Table 5: Relationship between Conformation Contents and Coordination Modes for Cu(II)−SF Complexes Prepared at Different pH Values with an Added Cu(II) Concentration of 1.8 mg of Cu/g of SF

	relevant conformation contents (%)					
pH	typical silk I	typical silk II	silk II related inter-mediate	silk I related inter-mediate	total silk II	coordination modes
8.0	67	12	13	8	25	Cu−4N
6.9	66	20	8	6	28	Cu−3N1O
5.2	52	33	9	6	42	Cu−2N2O (40%), Cu−1N3O (60%)[a]

[a] Summary of contents of component 2 and component 3 in Table 1. The relevant error in all reported contents is less than 2%.

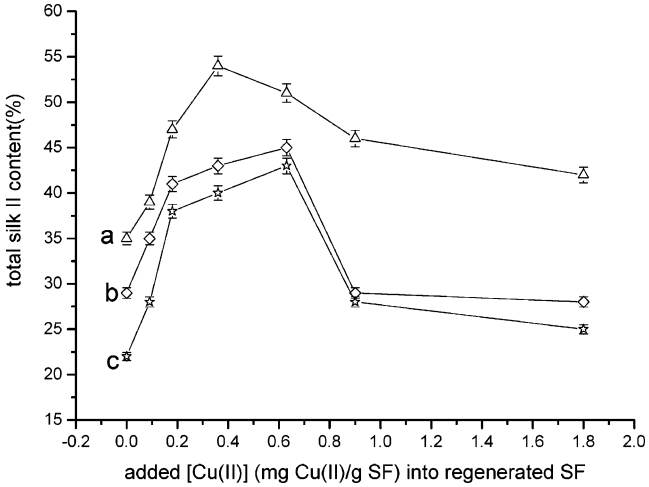

FIGURE 6: Dependence of total silk II conformations determined by ^{13}C CP-MAS NMR for the silk fibroin membranes on the prepared conditions at different Cu(II) concentrations and pH values. Curves a, b, and c represent total silk II conformation at pH 5.2, 6.9, and 8.0, respectively. The relevant error in all reported conformation contents is less than 2%.

β-sheet conformation; it was more characteristic of turns and loops at neutral and basic pH (*25*). Stöckel et al. also found that the binding of Cu(II) promoted the conformational shift of PrP from a soluble α-helical to an insoluble β-sheet-rich structure (*58*). Cu(II) in silk fibroin may also induce the formation of a β-form by the stable complex with amino acid residues via β-turn. However, such a type of coordination complex at neutral and basic pH may make the interaction between two β-form peptide chains more difficult, leading to a flexible macromolecular structure. On the other hand, under weakly acidic conditions (pH 5.2−4.0), an intermolecular His(N_τ)−Cu(II)−His(N_τ) bridge may be formed, inducing β-sheet formation and β-sheet aggregation and forming a rigid structure.

Cu(II)/Histidine Stoichiometry and SF Conformation. Although EPR-related parameter values, $g_{||}$ and $A_{||}$, show no obvious change with the variation of Cu(II) concentration at a pH of 5.2 or 4.0, a change is observed in the ratio of different coordination modes. In the heavy chain of *B. mori* SF, the ratio of the His residue in the AHGGYSGY peptides to the total amino acid residues (5263 residues) is only 5.7×10^{-4} (*19*). In addition, in the regenerated SF studied in this work, Cu(II) content of 0.018 mg of Cu/g of SF corresponding to a molar ratio of Cu(II) to total amino acid residues is 2.2×10^{-5} (taking into account the Cu atomic weight as 64 and the average molecular weight of every amino acid as 78). Therefore, the molar ratio of Cu(II) to the His residues in SF is very low (0.038:1) in the regenerated SF, predominated by random coil conformation. The added Cu(II) concentration of 0.09, 0.18, 0.36, 0.63, 0.9, and 1.8 mg of Cu/g of SF in the regenerated SF means that the molar ratios of Cu(II) to His increase gradually as 0.19:1, 0.38:1, 0.76:1, 1.33:1, 1.90:1, and 3.80:1 [ignoring the original Cu(II) content in SF, i.e., 0.018 mg of Cu/g of SF], respectively. Figure 6 represents the dependence of the total amount of silk II conformation extracted from the NMR spectra on the addition of Cu(II) at pH values of 5.2, 6.9, and 8.0, respectively. Interestingly, we find that a small amount of Cu(II) addition leads to an increase in the content of silk II conformation and that the content of total silk II is highest when the Cu(II) concentration is 0.36 mg of Cu/g of SF at a pH of 5.2; i.e., the molar ratio of Cu to His is 0.76:1, which matches with the qualitative observation in Raman spectra (Figure 4). Also, the content of total silk II is highest when the Cu(II) concentration is 0.63 mg of Cu/g of SF at pH values of 6.9 and 8.0; i.e., the molar ratio of Cu to His is 1.33:1. However, further addition of Cu(II) (≥0.63 mg of Cu/g of SF) results in a gradual reduction in the total silk II conformation content, but there is still more total silk II present in SF samples with added Cu(II) than that without added Cu(II). Notably, there is a similar trend at a pH of 5.2 between the Cu(II) coordination mode Cu−2N2O (Figure 3) and the SF conformation transition (Figure 6) when the Cu(II) concentration is increased. Figure 3 shows that the content of coordination mode Cu−2N2O is highest when the Cu(II) concentration is 0.36 mg of Cu/g of SF and that it also reduces upon further addition of Cu(II). This implies that the coordination mode Cu−2N2O may relate to the formation of silk II conformation, and the other coordination mode, Cu−1N3O (Figure 3), may lead to the formation of silk I conformation and/or silk I related intermediates.

We propose that Cu(II) binds with regenerated SF through the AHGGYSGY peptides at a pH of 5.2 via two modes, one is via a bridge of His(N_τ)−Cu(II)−His(N_τ) in which the ratio of Cu(II) to His is 0.5:1, and the other is via a mode of Cu−1N3O in which the ratio of Cu(II) to His is 1:1. Figure 6 shows that the silk II content is highest when the added Cu(II) concentration is 0.36 mg of Cu/g of SF at a pH of 5.2, which corresponds to a molar ratio of Cu(II) to His of about 0.76:1; this is very close to the ratio of 0.5:1 in the coordination mode His(N_τ)−Cu(II)−His(N_τ) if one considers that there may be a few Cu(II) ions in other coordination modes. Furthermore, the total silk II content at a pH of 5.2 gets to reduce above an added Cu(II) concentration of 0.63 mg of Cu/g of SF, which corresponds to a molar ratio of Cu(II) to His of 1.33:1; this is close to the ratio of 1:1 in the coordination modes of Cu−1N3O at a pH of 5.2 as well as Cu−3N1O at pH values of 6.9 and 8.0. Recently, we also investigated the interaction of cupric ions with silk fibroin in solution state by the neutral red (NR) fading method, one of the applications of UV spectrophotometry (*23*). The UV results indicate that Cu(II) is significantly bound onto SF macromolecular chains while the weight ratio of SF to Cu(II) is between 2500 and 25000; i.e., the molar ratio of Cu(II) to His is between 0.85:1 and 0.085:1. Hence, the Cu(II):AHGGYSGY stoichiometry at approximately 0.5:1 may be rationalized by considering that a small amount of Cu(II)

may efficiently induce the SF conformation transition from silk I to silk II via the formation of the Cu−2N2O coordination complex, while further addition of Cu(II) leads to an increase in other coordination complexes, thereby reducing the content of silk II. On the other hand, at pH 6.9 and 8.0, Cu(II) is more likely to bind SF as a coordination complex of Cu−3N1O or Cu−4N. In this way, the total silk II content is lower in neutral and basic pH values, and the optimum silk II content is reached at a higher added Cu(II) concentration of 0.63 mg of Cu/g of SF.

In conclusion, we find that the introduction of a small amount of Cu(II) induces the fractional changes of the conformational components of regenerated SF although the original concentration of Cu(II) is much lower than that of other metal elements, such as Ca(II) (1.040 ± 0.046 mg of Ca/g of SF) (*14*). This effect is possibly caused by the strong coordination ability of Cu(II) in biosystems. We demonstrated that the coordination modes and contents of Cu(II) in Cu(II)−SF complexes are pH- and Cu(II) concentration-dependent, and they are strikingly similar to those in the prion protein and Aβ peptides. Cu(II) may form a stable coordination with SF via the AHGGYSGY peptides in the heavy chain of *B. mori* silk fibroin. The predominant coordination modes observed are Cu−4N at a pH of 8.0, Cu−3N1O at a pH of 6.9, and Cu−2N2O and Cu−1N3O at a pH value of 5.2−4.0. At neutral and basic pH, the peptides AHGGYSGY in SF may likely form a 1:1 complex with Cu(II) by coordination via the imidazole N_π atom of His together with two deprotonated main-chain amide nitrogens in the two glycine peptides and one oxygen from the serine hydroxyl or from water. Such a type of coordination complex may make the interaction between two β-form peptide chains difficult, thereby leading to a flexible macromolecular structure. However, under weakly acidic conditions (pH 5.2−4.0), the Cu(II)−amide linkages may be broken and the metal binding site of His changes from N_π to N_τ to share a Cu(II) ion between two His residues in adjacent peptide chains. The formation of a Cu(II)−SF complex with a His(N_τ)−Cu(II)−His(N_τ) bridge may induce the β-sheet formation and further β-sheet aggregation, forming a rigid structure. Actually, silk fibroin is a very large polypeptide, whose structure is influenced by a number of factors. Among them, Cu and pH play some important role as discussed above. But the results reported here still need further validation. We are considering using model peptides derived from the silk fibroin sequence targeted by the Cu ions and more advanced analytical techniques. These results will be helpful for us to understand in depth the mechanism of the natural silk spinning process in the silkworm. Additionally, regenerated silk fibroin can be used as a suitable model to investigate other medical and clinical proteins, such as prion proteins and Aβ peptides, for diagnosis and drug development.

ACKNOWLEDGMENT

The ^{13}C solid-state NMR experiments in this work were performed in the State Key Laboratory of Magnetic Resonance and Atomic and Molecular Physics. We thank Prof. Chaohui Ye and Prof. Maili Liu at the State Key Laboratory for access to their InfinityPlus-400 NMR spectrometer and other facilities for experiments and Prof. Beat H. Meier at ETH Zurich and Dr. Ann Terry at Oxford University for helpful discussions.

REFERENCES

1. Kaplan, D., Adams, W. W., Farmer, B., and Viney, C. (1994) Silk—biology, structure, properties, and genetics, in *Silk Polymers. Materials Science and Biotechnology* (Kaplan, D., Adams, W. W., Farmer, B., and Viney, C., Eds.) Vol. 544, pp 2−16, American Chemical Society, Washington, DC.
2. Vollrath, F., and Knight, D. P. (2001) Liquid crystalline spinning of spider silk, *Nature 410*, 541−548.
3. Kerkam, K., Viney, C., Kaplan, D., and Lombardi, S. (1991) Liquid crystallinity of natural silk secretions, *Nature 349*, 596−598.
4. Calvert, P. (1998) Silk and sequence, *Nature 393*, 309−311.
5. Vollrath, F., Madsen, B., and Shao, Z. Z. (2001) The effect of spinning conditions on the mechanics of a spider's dragline silk, *Proc. R. Soc. London, Ser. B 268*, 2339−2346.
6. Madsen, B., and Vollrath, F. (2000) Mechanics and morphology of silk drawn from anesthetized spiders, *Naturwissenschaften 87*, 148−153.
7. Shao, Z. Z., and Vollrath, F. (2002) Surprising strength of silkworm silk—Silk fibers produced by artificial reeling are superior to those that are spun naturally, *Nature 418*, 741−741.
8. Magoshi, J., Magoshi, Y., Becker, M. A., and Nakamura, S. (1996) Biospinning (Silk Fiber Formation, Multiple Spinning Mechanisms), in *Polymeric Materials Encyclopedia* (Salamone, J. C., Ed.) pp 667−679, CRC Press, Boca Raton, FL.
9. Chen, X., Shao, Z. Z., Marinkovic, N. S., Miller, L. M., Zhou, P., and Chance, M. R. (2001) Conformation transition kinetics of regenerated *Bombyx mori* SF membrane monitored by time-resolved FTIR spectroscopy, *Biophys. Chem. 89*, 25−34.
10. Kobayashi, M., Tanaka, T., Inoue, S. I., Tsuda, H., Magoshi, J., Magoshi, Y, and Becker, M. A. (2001) Rheological behavior of silk fibroin aqueous solution: Gel-sol transition and fiber formation, *Polymer Prepr. 42*, 294−295.
11. Magoshi, J., Magoshi, Y., and Nakamura, S. (1994) Mechanism of fiber formation of silkworm, in *Silk Polymers. Materials Science and Biotechnology* (Kaplan, D., Adams, W. W., Farmer, B., and Viney, C., Eds.) Vol. 544, pp 292−310, American Chemical Society, Washington, DC.
12. Nam, J., and Park, Y. H. (2001) Morphology of regenerated silk fibroin: Effects of freezing temperature, alcohol addition, and molecular weight, *J. Appl. Polym. Sci. 81*, 3008−3021.
13. Motta, A., Fambri, L., and Migliaresi, C. (2002) Regenerated Silk Fibroin Films: Thermal and Dynamic Mechanical Analysis, *Macromol. Chem. Phys. 203*, 1658−1665.
14. Li, G. Y., Zhou, P., Sun, Y. J., Yao, W. H., Mi, Y., Yao, H. Y., Shao, Z. Z., and Yu, T. Y. (2001) The effect of metal ions on the conformation transition of silk fibroin, *Chem. J. Chin. Univ. 22*, 860−862.
15. Tsukada, M., Cotoh, Y., Nacura, M., Minoura, N., Kasai, N. A., and Freddi, G. (1994) Structural-changes of silk fibroin membranes induced by immersion in methanol aqueous-solutions, *J. Polym. Sci., Polym. Phys. 32*, 961−968.
16. Thiel, B. L., and Viney, C. (1997) Spider major ampullate silk (drag line): Smart composite processing based on imperfect crystals, *J. Microsc. 185*, 179−187.
17. Ishida, M., Asakura, T., Yokoi, M., and Saitô, H. (1990) Solvent- and mechanical-treatment-induced conformational transition of silk fibroins studied by high-resolution solid-state ^{13}C NMR spectroscopy, *Macromolecules 23*, 88−94.
18. Tanaka, T., Kobayashi, M., Tsuda, H., Inoue, S. I., Magoshi, Y., Nakamura, S., and Magoshi, J. (2002) Effect of inorganic salt on drawing of silk fibroin, *Polymer Prepr. 43*, 408−408.
19. Zhou, C. Z., Confalonieri, F., Medina, N., Zivanovic, Y., Esnault, C., Yang, T., Jacquet, M., Janin, J., Duguet, M., Perasso, R., and Li, Z. G. (2000) Fine organization of *Bombyx mori* fibroin heavy chain gene, *Nucleic Acids Res. 28*, 2413−2419.
20. Asakura, T., Sugino, R., Yao, J. M., Takashima, H., and Kishore, R. (2002) Comparative structure analysis of tyrosine and valine residues in unprocessed silk fibroin (silk I) and in the processed silk fiber (silk II) from *Bombyx mori* using solid-state ^{13}C, ^{15}N, and ^{2}H NMR, *Biochemistry 41*, 4415−4424.
21. Saitô, H., Iwanaga, Y., Tabeta, R., Narita, M., and Asakura, T. (1983) A high resolution ^{13}C NMR study of silk fibroin in solid state by the cross polarization-magic angle spinning method: conformational characterization utilizing conformation-dependent ^{13}C chemical shifts, *Chemistry Lett.*, 427−430.
22. Hossain, K. S., Ochi, A., Ooyama, E., Magoshi, J., and Nemoto, N. (2003) Dynamic light scattering of native silk fibroin solution

extracted from different parts of the middle division of the silk gland of the *Bombyx mori* silkworm, *Biomacromolecules 4*, 350−359.
23. Zhou, L., Chen, X., Shao, Z. Z., Zhou, P., Knight, D. P., and Vollrath, F. (2003) Copper in the silk formation process of *Bombyx mori* silkworm, *FEBS Lett. 554*, 337−341.
24. Li, G. Y., Zhou, P., Shao, Z. Z., Xie, X., Chen, X., Wang, H. H., Chunyu, L. J., and Yu, T. Y. (2001) The natural silk spinning process−A nucleation-dependent aggregation mechanism, *Eur. J. Biochem. 268*, 6600−6606.
25. Viles, J. H., Cohen, F. E., Prusiner, S. B., Goodin, D. B., Wright, P. E., and Dyson, H. J. (1999) Copper binding to the prion protein: Structural implications of four identical cooperative binding sites, *Proc. Natl. Acad. Sci. U.S.A. 96*, 2042−2047.
26. Aronoff-Spencer, E., Burns, C. S., Avdievich, N. I., Gerfen, G. J., Peisach, J., Antholine, W. E., Ball, H. L., Cohen, F. E., Prusiner, S. B., and Millhauser, G. L. (2000) Identification of the Cu^{2+} binding sites in the N-terminal domain of the Prion Protein by EPR and CD spectroscopy, *Biochemistry 39*, 13760−13771.
27. Cereghetti, G. M., Schweiger, A., Glockshuber, R., and Doorslaer, S. V. (2001) Electron paramagnetic resonance evidence far binding of Cu^{2+} to the C-terminal domain of the murine prion protein, *Biophys. J. 81*, 516−525.
28. Miura, T., Hori-I, A., Mototani, H., and Takeuchi, H. (1999) Raman spectroscopic study on the copper(II) coordination mode of prion octapeptide and its pH dependence, *Biochemistry 38*, 11560−11569.
29. Millhauser, G. L. (2004) Copper binding in the prion protein, *Acc. Chem. Res. 37*, 79−85.
30. Miura, T., Suzuki, K., Kohata, N., and Takeuchi, H. (2000) Metal coordination modes of Alzheimer's amyloid β-peptide in insoluble aggregates and soluble complexes, *Biochemistry 39*, 7024−7031.
31. Atwood, C. S., Moir, R. D., Huang, X., Scarpa, R. C., Bacarra, N. M., Romano, D. M., Hartshorn, M. A., Tanzi, R. E., and Bush, A. I. (1998) Dramatic aggregation of Alzheimer Aβ by Cu(II) is induced by conditions representing physiological acidosis, *J. Biol. Chem. 273*, 12817−12826.
32. Yen, T. F. (1969) *Electron spin resonance of metal complexes*, Plenum Press, New York.
33. Asakura, T., and Yao, J. M. (2002) ^{13}C CP/MAS NMR study on structural heterogeneity in *Bombyx mori* silk fiber and their generation by stretching, *Protein Sci. 11*, 2706−2713.
34. Asakura, T., Yao, J. M., Yamane, T., Umemura, K., and Ulrich, A. S. (2002) Heterogeneous structure of silk fibers from *Bombyx mori* resolved by ^{13}C solid-state NMR spectroscopy, *J. Am. Chem. Soc. 124*, 8794−8795.
35. Peisach, J., and Blumber, W. E. (1974) Structural implications derived from the analysis of electron paramagnetic resonance spectra of natural and artificial copper proteins, *Arch. Biochem. Biophys. 165*, 691−707.
36. Lin, Q. S. (1989) The relation between the magnetic parameters $g_{||}$ and $A_{||}$ for Cu(II) complexes, *Chin. J. Magn. Reson. 6*, 201−208.
37. Swartz, H. M., Bolton, J. R., and Borg, D. C. (1972) *Biological Application of Electron Spin Resonance*, Wiley-Interscience, New York.
38. Sakaguchi, U., and Addison, A. W. (1979) Spectroscopic and redox studies of some copper(II) complexes with biomimetic donor atoms: implications for protein copper centers, *J. Chem. Soc., Dalton Trans. 4*, 600−608.
39. McGarvey, B. R. (1966) *Transition Metal Chemistry* (Carlin, R. L., Ed.) Vol. III, p 90, Marcel Dekker, New York.
40. Gersmann, H. R., and Swalen, J. D. (1962) Electron paramagnetic resonance (E. P. R.) spectra of copper complexes, *J. Chem. Phys. 36*, 3221−3233.
41. Kubelka, J., Pancoska, P., and Keiderling, T. A. (1999) Novel use of a static modification of two-dimensional correlation analysis. Part II: Hetero-spectral correlations of protein Raman, FT-IR, and circular dichroism spectra, *Appl. Spectrosc. 53*, 666−671.
42. Yeo, S. D., Debenedetti, P. G., Patro, S. Y., and Przybycien, T. M. (1994) Secondary structure characterization of microparticulate insulin powders, *J. Pharm. Sci. 83*, 1651−1656.
43. Thomas, G. J., and Kyogoku, Y. (1977) Biological Science, in *Infrared and Raman Spectroscopy (Part C)* (Brame, E. G., and Grasselli, J. G., Eds.) Marcel Dekker, New York.
44. Lippert, J. L., Tyminski, D., and Desmeules, P. J. (1976) Determination of the secondary structure of proteins by Laser Raman spectroscopy, *J. Am. Chem. Soc. 98*, 7075−7080.
45. Edwards, H. G. M., and Farwell, D. W. (1995) Raman-spectroscopic studies of silk, *J. Raman Spectrosc. 26*, 901−909.
46. Monti, P., Freddi, G., Bertoluzza, A., Kasai, N., and Tsukada, M. (1998) Raman spectroscopic studies of silk fibroin from *Bombyx mori*, *J. Raman Spectrosc. 29*, 297−304.
47. Ochsenfeld, C., Brown, S. P., Schnell, I., Gauss J., and Spiess, H. W. (2001) Structure assignment in the solid state by the coupling of quantum chemical-calculations with NMR experiments: A columnar hexabenzocoronene derivative, *J. Am. Chem. Soc. 123*, 2597−2606.
48. Spera, S., and Bax, A. (1991) Empirical correlation between protein backbone conformation and C-alpha and C-beta ^{13}C nuclear-magnetic-resonance chemical-shifts, *J. Am. Chem. Soc. 113*, 5490−5492.
49. Saitô, H., Tabeta, R., Shoji, A., Ozaki, T., and Ando, I. (1983) Conformational characterization of polypeptides in the solid-state as viewed from the conformation-dependent ^{13}C chemical-shifts determined by the ^{13}C cross polarization magic angle spinning method: Oligo(L-alanine), poly(L-alanine), copolymers of L-alanine and D-alanine, and copolymers of L-alanine with *N*-methyl-L-alanine or *N*-benzyl-L-alanine, *Macromolecules 16*, 1050−1057.
50. Asakura, T., Ashida, J., Yamane, T., Kameda, T., Nakazawa, Y., Ohgo, K., and Komatsu, K. (2001) A repeated β-turn structure in poly(Ala-Gly) as a model for silk I of *Bombyx mori* silk fibroin studied with two-dimensional spin-diffusion NMR under off magic angle spinning and rotational echo double resonance, *J. Mol. Biol. 306*, 291−305.
51. Rao, B. K. S., Tyryshkin, A. M., Roberts, A. G., Bowman, M. K., and Kramer, D. M. (2000) Inhibitory copper binding site on the spinach cytochrome b(6)f complex: Implications for Q(0) site catalysis, *Biochemistry 39*, 3285−3296.
52. Liu, G. F., Ghen, W. X., Fu, Y. Q., and Shen, Z. Q. (2001) Coordination reaction of silk sericin protein with copper (II), *Acta Polym. Sin. 1*, 58−61.
53. Hojo, N., Shirai, H., and Takayama, K. (1969) Effect of cupric cations on the conformation of silk fibroin, *Kogyo Kagaku Zasshi 72*, 470−473.
54. Shimizu, F., Zoku, K. K., and Shinkyo, I. (1980) Adsorption behaviors of metal ions on silk and their effect on the photo-degradation of the silk, *Zoku Kenshi no Kozo*, 485−497.
55. Chen, W. X., Shen, Z. Q., Liu, G. F., and Shirai, H. (2000) Coordination structure and higher order structure of Cu(II)-silk fibroin protein (*Bombyx mori*) complexes, *Chem. J. Chin. Univ. 21*, 306−310.
56. Luo, J. X., and Zhang, N. Z. (1987) *Introduction of Bioinorganic Chemistry* (Chinese), pp 1−572, Chemical Industry Press [translated from *Bioinorganic Chemistry, An Introduction* (Ochiai, E. I., Ed.) Allyn and Bacon, Inc.].
57. Schlick, S. (1986) Binding-sites of Cu(II) in chitin and chitosan: an electron spin resonance study, *Macromolecules 19*, 192−195.
58. Stöckel, J., Safar, J., Wallace, A. C., Cohen, F. E., and Prusiner, S. B. (1998) Prion protein selectively binds copper(II) ions, *Biochemistry 37*, 7185−7193.
59. Riek, R., Hornemann, S., Wider, G., Glockshuber, R., and Wuthrich, K. (1997) NMR characterization of the full-length recombinant murine prion protein, mPrP(23−231), *FEBS Lett. 413*, 282−288.
60. Donne, D. G., Viles, J. H., Groth, D., Mehlhorn, I., James, T. L., Cohen, F. E., Prusiner, S. B., Wright, P. E., and Dyson, H. J. (1997) Structure of the recombinant full-length hamster prion protein PrP(29−231): The N terminus is highly flexible, *Proc. Natl. Acad. Sci. U.S.A. 94*, 13452−13457.
61. Goldmann, W., Hunter, N., Martin, T., Dawson, M., and Hope, J. (1991) Different forms of the bovine PrP gene have 5 or 6 copies of a short, G-C-rich element within the protein-coding exon, *J. Gen. Virol. 72*, 201−204.
62. Van Doorslaer, S., Cereghetti, G. M., Glockshuber, R., and Schweiger, A. (2001) Unraveling the Cu^{2+} binding sites in the C-terminal domain of the murine prion protein: A pulse EPR and ENDOR study, *J. Phys. Chem. B 105*, 1631−1639.

BI049455H